RSC Advances

ROYAL SOCIETY OF CHEMISTRY

www.rsc.org/advances

Novel aromatic polyimides derived from 2,8-di(3-aminophenyl)dibenzofuran. Synthesis, characterization and evaluation of properties

Alain Tundidor-Camba[a*]; Claudio A. Terraza[a]; Luis H. Tagle[a]; Deysma Coll[a]; Pablo Ortiz[a], Javier de Abajo[b]; Eva M. Maya[b]

[a]Organic Chemistry Department, Faculty of Chemistry, Pontificia Universidad Católica de Chile, Box 306, Post 22, Santiago, Chile.

[b]Instituto de Ciencia y Tecnología de Polímeros, CSIC, Juan de la Cierva 3, 28006 Madrid, Spain

*Corresponding author. Tel.: +56223541199. E-mail address: atundido@uc.cl

ABSTRACT

Three aromatic polyimides (**PIs**) were prepared from a new aromatic diamine monomer derived from the rigid ring dibenzofuran. All **PIs** were obtained in high yield and the inherent viscosities were in the range of 0.60 and 0.74 dL/g. Polyimides derived from 4,4'-hexafluoroisopropyliden diphthalic anhydride (**6FDA**) and 4,4'-(dimethylsilanediyl) diphthalic anhydride (**SiDA**) showed excellent solubility in a variety of aprotic polar organic solvents. All **PIs** showed high thermal stability with thermal decomposition temperature ($TDT_{10\%}$) between 555-590ºC and the glass transition temperatures (Tg) values were between 290 and 315 °C. Polymeric films were obtained from **PI-6FDA** and **PI-SiDA** solutions and then contact angle and surface free energy were tested in order to know the hydrophobicity of materials. Likewise, permeability and selectivity analyses were developed where **PI-6FDA** film offered a reasonably acceptable balance of permselectivity with values close to the Robeson upper-bound (1991), in particular for the CO_2/CH_4 gas pair.

Keywords: aromatic polyimides, gas separation membrane, contact angle and thermal stability.

1. Introduction

Aromatic polyimides are materials having excellent thermal, mechanical and chemical properties. Its use is in various areas such as, in the manufacture of household appliances, textiles, insulation, implants, optoelectronics and gas separation, among others. However, fully aromatic polyimides are insoluble in organic solvents, limiting their processability[1-4]. Therefore, efforts have been made to chemically modify the composition of classical polyimides to make them more easily processable, and many examples have been reported in the last two decades of aromatic polyimides which are amorphous at room temperature and soluble in organic polar solvents[5-8].

Glassy aromatic polymers are preferred to be tested as candidates for gas separation as they usually show high glass transition temperatures, well over 200 ^{o}C, what assures glassy state and absence of crystallinity at the usual temperatures for gas separation operations, and they have also good thermal resistance, good mechanical properties and processability. In this regard, soluble, glassy polyimides have been the object of numerous studies as they exhibit a combination of structural features particularly favourable to provide high fractional free volume and molecular stiffness at the same time[9-12].

So, several structural modifications can be incorporated into the design of diamine or dianhydride monomers to decrease the molecular packing and thereby the interactions between the polymer chains. Incorporating flexible segments, bulky groups, monomers with *meta* substituents, sp3 centers that allow free rotation and even the replacement of carbon per silicon are some modifications made by various researchers[13-16]. Introduction of diphenylsilane units in the polymer backbone improves the solubility and maintains the thermal properties of the polymeric materials[17, 18].

These chemical modifications provide chain separation, and consequently, higher free volume and solubility, without affecting the thermal properties[19-20]. Alternatively, soluble aromatic polyimides can be obtained from non-planar monomers, where the non-planarity decreases the chain regularity order[21, 22]. Biphenyl based monomers are considered non-planar and the free rotation is somewhat prevented, increasing the rigidity to the system. It is a desirable property for gas separation applications besides high thermal resistance, high glass-transition temperatures (Tg), and good mechanical properties[23].

This article reports the synthesis and characterization of a novel aromatic diamine with biphenyl units and *meta* substitutions on the structure. It has been prepared by Suzuki-Miyaura methodology [24]. Polycondensation of this diamine with three aromatic dianhydrides, one of them containing a dimethyldiphenylsilane unit were carried out. Structural characterization of the resulting polyimides, and evaluation of properties such as solubility, angle contact, surface free energy, inherent viscosity, thermal behavior and gas separation ability were also investigated and discussed.

2. Experimental

2.1. Materials

Anhydrous *N,N*-dimethylacetamide (DMAc), anhydrous pyridine (Py), acetic anhydride, 3-nitrophenylboronic acid, hydrazine monohydrate (80 %), Pd/C (10 % w/w), bis(triphenylphosphine)palladium (II) dichloride, 4,4'-hexafluoroisopropyliden diphthalic anhydride (**6FDA**) and benzophenone-3,3′,4,4′-tetracarboxylic anhydride (**BTDA**) were obtained from Aldrich Chemical (Milwaukee, WI). Both dianhydrides were sublimated before used. 4,4'-(dimethylsilanediyl) diphthalic anhydride (**SiDA**) and 2,8-diiododibenzofuran were synthesized following a procedure already reported in the literature[25, 26]. All other reagents and solvents were purchased commercially as analytical-grade and used without further purification.

2.2. Instrumentation and measurements

FT-IR spectra (KBr pellets) were recorded on a Perkin-Elmer (Fremont CA) 1310 spectrophotometer over the range of 4000-450 cm^{-1}. Melting points (uncorrected) were obtained on a SMP3 Stuart Scientific melting point apparatus. ^{1}H, ^{13}C and ^{29}Si NMR spectra were carried out on a 400 MHz instrument (Bruker AC-200) using DMSO-d_6 as solvent and TMS as internal standard. Viscosimetric measurements were made in a Desreux-Bischof type dilution viscosimeter at 25 °C (c = 0.5 g/dL). Glass transition temperature (Tg) values were obtained with a Mettler-Toledo (Greifensee, Switzerland) DSC 821 calorimetric system from second run (10 ºC/min under N_2 flow). Thermogravimetric analyses were carried out in a Mettler (Switzerland) TA-3000 calorimetric system equipped with a TC-10A processor, and a TG-50 thermobalance with a Mettler MT5 microbalance (temperature range between 25 ºC and 900 ºC at 10 ºC/min under N_2 flow). Elemental analyses were made on a Fisons EA 1108-CHNS-O equipment. A Dataphysics OCA 20 device with a conventional goniometer and high performance video camera, controlled by SCA20 software was used to measure the optical contact angle and surface free energy. Permeability to pure gases was studied on polymer films, made by casting 10% (w/v) DMAc solutions of polymers onto a leveled glass plate and by heating at 80 °C for 12 h and at 180 °C under vacuum overnight. A barometric method was used to determine steady-state pure gas permeability at 30 °C, applying a pressure of 3 bar and an initial pressure in the expansion chamber < 0.1 mbar. For the permeation experiments, high purity oxygen, nitrogen, methane and carbon dioxide were used. Permeability values (P) were determined from the slope of downstream pressure versus time, plotted once steady state had been achieved, according to the expression:

$$P = K\,(BxL)/P_0$$

where K is an apparatus constant that includes parameters such as temperature, cell permeation area and volume of the system, B is the slope of downstream pressure versus time, L is the film thickness and P_0 is the upstream pressure. The ideal separation factors were calculated from the ratio of permeability coefficients:

$$\alpha_{A/B} = P_A/P_B$$

where P_A and P_B refer to the permeability coefficients of pure gases A and B, respectively. To ensure reproducibility of results and to check the membrane homogeneity, two disks of the membrane were measured.

2.3. Monomer synthesis and characterization

2,8-di(3-nitrophenyl)dibenzofuran (**1**). In a 50 mL, round-bottomed flask, 2,8-diiododibenzofuran (10.0 mmol), 3-nitrophenylboronic acid (23.0 mmol), bis(triphenylphosphine)palladium (II) dichloride (1.5 mmol), 1,4-dioxane (30 mL) and potassium carbonate solution (30 mL, 2 M) were added. The suspension was heated at 95 °C for 24 hours with stirring and nitrogen atmosphere. The mixture was allowed to reach room temperature and then was poured into 500 mL of distilled water with stirring. The precipitated brown powder was collected by filtration, washed thoroughly with distilled water and acetone, and dried. The crude product was recrystallized from DMF-EtOH mixture (1.5:1 vol/vol) to obtain yellow crystals.

Yield: 95 %. M.p.: 267 - 268 °C. IR (KBr, cm^{-1}): 3081 (C-H arom.); 1595, 1474 (C=C); 1516, 1345 (NO_2); 1202 (C-O-C); 807, 681 (*m*-subst. arom.). The solution characterization was not performed due to the insolubility of the compound in all tested deuterated solvents (DMSO-d_6, Acetone-d_6 and $CDCl_3$). Elem. Anal. Calcd. for. $C_{24}H_{14}N_2O_5$; (410.38): C, 70.24 %; H, 3.44 %, N, 6.83 %. Found: C, 70.15 %; H, 3.34 %, N, 6.75 %.

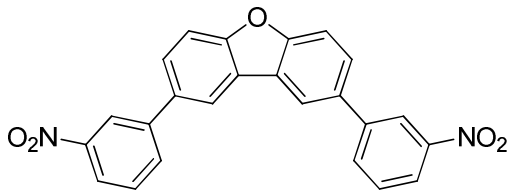

2,8-di(3-aminophenyl)dibenzofuran (**2**). A mixture of 2,8-di(3-nitrophenyl)dibenzofuran (**1**) (10.0 mmol), 0.35 g of palladium on activated carbon at 10 wt. % and 50 mL of absolute ethanol was placed into a 100 mL three-necked flask fitted with magnetic stirrer, condenser and a dropping funnel. The system was heated to reflux and 15 mL of hydrazine monohydrate was added dropwise over a period of 1.5 hours. After the addition, the mixture was refluxed for 24 hours. The mixture was filtered and the solution was poured into 800 mL of water with stirring. A white solid was obtained, which was filtered and dried at room temperature for 12 h. The crude precipitate was recrystallized from EtOH to obtain white crystals.

Yield: 75 %. M.p.: 180 - 182 °C. IR (KBr, cm^{-1}): 3389, 3300, 3200 (N-H stretching), 3038 (C-H arom.); 1604 (N-H flexion), 1581, 1478, 1465 (C=C); 1195 (C-O-C); 810, 696 (*m*-subst. arom.). ^{1}H NMR (DMSO-d_6, δ, ppm): 8.30 (s, 2H(12)); 7.56 (s, 4H(8,9)); 7.02 (t, J = 7.8, 2H(3)); 6.88 (s, 2H(6)); 6.78 (d, J = 7.6 Hz, 2H(4)); 6.50 (d, J = 7.9 Hz, 2H(2)); 5.05 (s, 4H(13)). ^{13}C NMR

(DMSO-d_6, δ, ppm), 155.4 (C10), 149.1 (C1), 141.0 (C5), 136.6 (C8), 129.5 (C7), 126.3 (C3), 124.2 (C11), 119.1 (C12), 114.9 (C4), 113.0 (C2), 112.6 (C6), 111.7 (C9). Elem. Anal. Calcd. for. $C_{24}H_{18}N_2O$; (350.41): C, 82.26 %; H, 5.18 %, N, 7.99 %. Found: C, 82.18 %; H, 5.15 %, N, 7.83 %.

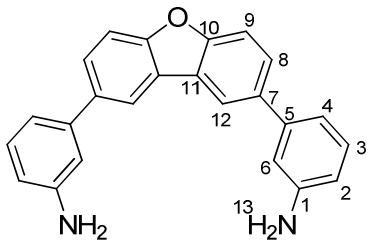

2.4. Polymer synthesis and characterization

A typical polymerization procedure for the synthesis of the polyimides was as follows. To a three-necked round-bottomed flask equipped with mechanical stirrer and nitrogen atmosphere, a mixture of 2.0 mmol of the diamine (**2**), 2.0 mmol of the corresponding dianhydride and 4 mL of DMAc was added and stirred at room temperature during 6 hours. After that, 1.0 mL of acetic anhydride and 0.8 mL of pyridine were added and the mixture was stirred for two hours at room temperature and then another hour at 60 °C. Then, the mixture was cooled and poured in 300 mL of water with stirring. The white solid was filtered, washed thoroughly with methanol and dried at 100 °C during 12 hours.

PI-6FDA: Yield: 99 %. IR (KBr, ν, cm^{-1}), 3068 (C-H arom.); 1775, 1711 (C=O); 1606, 1543 (C=C); 1120 (C-O-C); 815, 690 (*m*-subst. arom.). ^{1}H NMR (DMSO-d_6, δ, ppm), 8.43 (s, 2H(4)); 8.16 (s, 2H(22)); 7.97 (s, 2H(12)); 7.79 (m, 12H(7,8,15,16,18,19)); 7.72 (s, 2H(14)). ^{13}C NMR (DMSO-d_6, δ, ppm), 166.4 (C9); 166.3 (C10); 156.0 (C20); 147.1 (C8); 141.1 (C13); 137.7 (C5); 136.1 (C3); 134.8 (C11); 133.3 (C6); 132.9 (C18); 132.7 (C17); 132.1 (C15); 129.9 (C2); 127.0 (C12); 126.2 (C21); 126.1 (C4); 124.6 (C22); 124.0 (C16); 122.8 (C14); 119.8 (C7); 112.5 (C19); 68.7 (C1). Elem. Anal. Calcd. for $[C_{43}H_{20}F_6N_2O_5]_n$ $(758.62)_n$, C, 68.08 %; H, 2.66 %; N, 3.69 %. Found: C, 67.99 %; H, 2.43 %; N, 3.56 %.

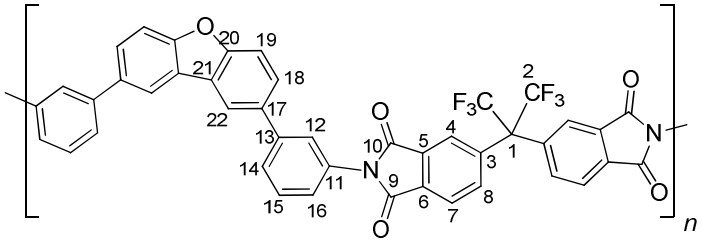

PI-BTDA: Yield: 98 %. IR (KBr, ν, cm^{-1}), 3060 (C-H arom.); 1778, 1720 (C=O); 1602, 1579, 1476 (C=C); 1119 (C-O-C); 813, 696 (*m*-subst. arom.). The solution characterization was not performed due to the insolubility of the compound in all tested deuterated solvents (DMSO-d_6, Acetone-d_6 and $CDCl_3$). Elem. Anal. Calcd. for $[C_{41}H_{20}N_2O_6]_n$ $(636.61)_n$, C, 77.35 %; H, 3.17 %; N, 4.40 %. Found: C, 77.15 %; H, 3.09 %; N, 4.29 %.

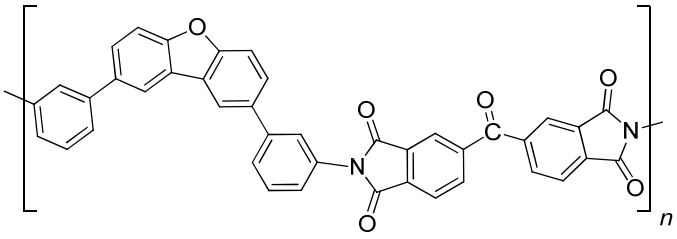

PI-SiDA: Yield: 99 %. IR (KBr, ν, cm^{-1}), 3058 (C-H arom.); 2955 (C-H aliph.); 1776, 1715 (C=O) 1606, 1581 (C=C); 1408, 1065 (Si-C arom.); 1371 (Si-C aliph); 1118 (C-O-C); 812, 695 (*m*-subst. arom.). ^{1}H NMR (DMSO-d_6, δ, ppm), 8.51 (s, 2H(4)); 8.08 (s, 4H(12,22)); 7.77 (s, 12H(7,8,15,16,18,19)); 7.39 (s, 2H(14)); 0.71 (s, 6H(2)). ^{13}C NMR (DMSO-d_6, δ, ppm), 167.5 (C9); 167.3 (C10); 156.2 (C20); 146.1 (C8); 141.2 (C13); 140.7 (C5); 136.6 (C3); 135.1 (C11); 133.0 (C6); 131.2 (C18); 129.9 (C17); 128.7 (C15); 128.0 (C2); 127.1 (C12); 126.9 (C21); 126.3 (C4); 126.2 (C22); 124.8 (C16); 123.1 (C14); 119.8 (C7); 112.5 (C19); -2.7 (C2). ^{29}Si NMR (DMSO-d_6, δ, ppm), -8.05. Elem. Anal. Calcd. for $[C_{42}H_{26}N_2O_5Si]_n$ $(666.75)_n$, C, 75.66 %; H, 3.93 %; N, 4.20 %. Found: C, 75.56 %; H, 3.85 %; N, 4.11 %.

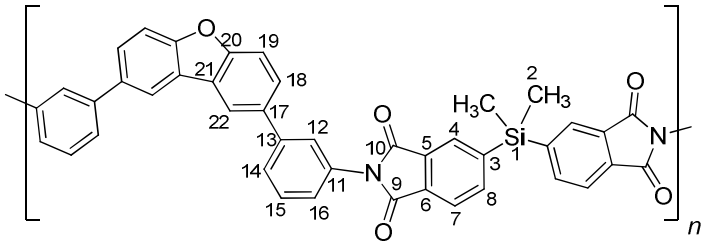

3. Results and discussion

3.1. Monomer synthesis

The diamine containing biphenyl units was obtained by following the methodology developed by Suzuki-Miyaura, which consisted of a carbon-carbon coupling reaction, using a halogen derivative, a boronic acid derivative and a palladium catalyst, in the presence of a base. In this case, the

halogenated compound was 2,8-diiododibenzofuran and the boronic acid derivative was 3-nitrophenylboronic acid, which rendered the corresponding dinitro intermediate in 95% yield (Scheme 1).

Scheme 1. Here

The solution characterization was not possible due to their insolubility in the tested deuterated solvents, however, FT-IR spectrum clearly showed the signals corresponding to the general structure included the N=O stretching bands at 1516 and 1345 cm^{-1} of the nitro group (Fig 1). The reduction reaction of dinitro compound with hydrazine monohydrate in the presence of palladium supported on activated carbon produced the desired diamine monomer **(2)** in high yield (75%), which was finally recrystallized from ethanol. The FT-IR spectrum of the diamine confirmed its structure as N-H stretching bands could be identified at 3389, 3300 and 3200 cm^{-1} and the N-H flexion band at 1604 cm^{-1}. Likewise, the stretching bands associated to the nitro group are not present in the new spectrum.

Figure 1. Here

Fig. 2 shows the ^{1}H and ^{13}C NMR spectra of diamine (**2**) in DMSO-d_6. The singlet at 8.30 ppm corresponds to hydrogens H12, which are more displaced to low magnetic field due to the mesomeric effect (-M) of the neighboring aromatic ring. H8 and H9 hydrogens have the same chemical shift due both to the mesomeric effect of the neighbor aromatic ring and the inductive effect of the oxygen atom. The singlet at 5.05 ppm corresponds to the hydrogens of the amino group, which are magnetically equivalent due to the symmetry of the structure.

Figure 2. Here

Meanwhile, the ^{13}C NMR spectrum showed the twelve expected aromatic signals. The signals shifted to low magnetic field corresponded to the carbons C10 and C1, because the electronic influence of the N and O atoms directly bonded to them.

3.2. Polymer synthesis

Three new aromatic polyimides were synthesized by a conventional two-step procedure, reacting the appropriate dianhydride with 2,8-di(3-aminophenyl)dibenzofuran (**2**) in DMAc as solvent, at room temperature for 6 hours (Scheme 2). All polyamic acids were soluble in the reaction media,

however, when the chemical cyclization was made, only **PI-6FDA** and **PI-SiDA** were soluble in DMAc.

Scheme 2. Here

Successful conversion from polyamic acid to polyimide was confirmed by the FT-IR spectra, in which the characteristic absorption bands due to the symmetric and asymmetric stretching of the carbonyl group around 1780 and 1720 cm^{-1} (υC=O) can be clearly identified (See Experimental Part). As an example, the FT-IR spectrum of **PI-SiDA** has been reproduced in Fig. 3.

Figure 3. Here

Fig 4 shows the ^{1}H and ^{29}Si NMR spectra of **PI-SiDA.** The assignments of each hydrogen designated are in full agreement with the proposed polymer structures. The signal at high field corresponds to the hydrogens H2 of the dianhydride moiety. These nucleus are strongly shifted to high magnetic field due to the lower electronegativity of the silicon atom respect to a carbon one. In the ^{29}Si NMR spectrum, only one signal at -8.05 ppm was observed. This chemical shift is expected when the silicon atom is surrounded by two aromatic rings and two methyl groups[27, 28].

Figure 4. Here

3.3. Inherent viscosity and solubility

Inherent viscosity was measured at a single point, in *N*-methyl-2-pyrrolidone (NMP) solution at 25 ± 0.1 °C (0.5 g/dL). **PI-SiDA** and **PI-6FDA** had high inherent viscosity values (0.74 and 0.60 dL/g, respectively), indicating high molecular weight (Table 1). For **PI-BTDA,** it was not possible to measure this property due to its insolubility in all tested organic solvents, including concentrated sulfuric acid. In this sense, the solubility of the polyimides was analyzed in a series of common organic solvents. Thus, **PI-SiDA** and **PI-6FDA** were soluble at room temperature in DMSO, NMP, DMF, DMAc and *m*-cresol. Both samples were insoluble even with application of temperature (about 40 °C) in THF.

Table 1. Here

Usually, polyimides derived from anhydride 6FDA have good solubility in aprotic polar solvents due to the polarity of the CF_3 group and the big free volume caused by this group, which increases

the inter-chains distance[29-31]. On the other hand, the excellent solubility of **PI-SiDA** in the same solvents could be related with the presence of the silicon atom as central element on the anhydride fragment.

The silicon atom is bigger than carbon atom causing major bond distances, which increases the free rotation. Additionally, the methyl groups bonding on silicon atom increase the inter-chain distance. Basically, both anhydrides have similar structures in contrast to anhydride BTDA. The ketone carbonyl group at the center of the structure has planar molecular geometry, allowing the approach of the polymeric chains, which increases the intermolecular charge transfer. The molecular interactions in **PI-BTDA** are the biggest, thereby decreasing strongly their solubility.

3.4. Thermal properties

Thermal stability of all polyimides was evaluated by TGA and DSC techniques under a nitrogen atmosphere and the results are summarized in Table 2. Fig. 5 shows the TGA curves for all **PIs**. The samples exhibited good thermal stability, with the 10 % weight loss temperature ($TDT_{10\%}$) over 550 °C, which allow them to be classified as thermally stable.

Table 2. Here

PI-BTDA exhibited the highest thermal stability among them, probably due to the absence of sp3 hybridized carbons. The weight residues at 800 °C were greater than 45 % in all cases. This fact could be related to the inert atmosphere used in the analyses and the high aromatic content of all samples. **PI-SiDA** showed the highest value, which can be attributed mainly to silicon oxides formed at the calcination temperature.

Figure 5. Here

DSC analyses were performed in order to obtain the Tg value of all polyimides and the results are summarized in table 2. Polymers did not show any melting endotherm, indicating the amorphous nature of the materials. Only one thermal transition was detected in all polyimides, corresponding to the Tg. **PIs** showed high Tg values, greater than 290 °C. The significantly high Tg of **PI-6FDA** (315°C) is common in 6FDA-based polyimides[32-35]. The introduction of the -$C(CF_3)_2$- linkage restricts the torsional motion of neighboring phenyl rings and tends to increase rigidity. On the other hand, **PI-SiDA** has the lower Tg value, which is in agreement with presence of the silicon atom in the polymer main chain. This structural element increases the possibility of torsional motion

through the chain, which increases flexibility. The effect of the great Si-C distance bond respect to a C-C one was before discussed for explaining the results of solubility.

PI-BTDA has higher Tg value than **PI-SiDA** due to the planarity of the ketone group in the anhydride fragment, which causes that the chains come closer in **PI-BTDA**, increasing structural rigidity and molecular packing. Basically, the Tg values were consistent with the structural design of each polymer.

3.5. Contact angle and surface free energy

Dense films were prepared from **PI-6FDA** and **PI-SiDA** by casting 10 % (w/v) filtered DMAc polymer solutions onto a glass plate and heating at 60 °C overnight. Then, the films were stripped off and were dried in a vacuum oven at 100 °C overnight and at 150 °C for 48 h. The contact angle on the films both for water (θ_w) and for toluene (θ_t) are given at table 3 and the image of the drop (Fig. 6) was captured five seconds after placed.

Table 3. Here

PI-SiDA showed much higher contact angles compared with **PI-6FDA**. This result indicated that the silylated film is more hydrophobic than that of **PI-6FDA**. According with previous reports, the silicon based polymers are characterized by high hydrophobicity[36]. With the contact angle values, the surface free energy (σ) of both films was calculated using a model previously described[37, 38]. Also, the dispersive (σ_d) and polar (σ_p) components were determined and all results are shown in table 3. As can be seen, the surface free energy of both films are similar, however, the component parameters not. According to these values, the polar groups (imide, ether and CF_3) and the hydrocarbon backbone are uniformly oriented toward the surface of the film, since the values of both components are nearby. In the silylated film, the polar component plays an important role because, apart from the imide and ether groups, also C-Si bonds generated higher polarity at the polymer backbone[16]. The proximity to the surface of the silicon atom generates greater hydrophobicity, agreeing with the results of contact angle observed.

Figure 6. Here

3.6. Gas transport properties

6FDA-based polyimides have been widely used as membrane in the field of gas separation, due to its excellent separation characteristics at low pressures for several gas pairs[31]. In this work, a preliminary study about gas permeability capacity through the **PI-6FDA** film was made. The results are listed in table 4. For comparative purposes, the permeability and ideal separation factors for other polyimides, one of them commercial polyimide (Matrimid), have also been included[23, 39-41].

Table 4. Here

The permeability coefficients to O_2, N_2, CH_4 and CO_2 obtained for **PI-6FDA** were lower that the reported **6FDA-TBAPB** and similar to those reported for commercial polyimide, Matrimid. However to evaluate the performance of the novel polyimide, the O_2 and CO_2 permeabilities were plotted versus O_2/N_2 and CO_2/CH_4 selectivities in a Robeson type diagram (Figure 7) were the best polymer for this separation is characterized by the upper bound line established by Robeson[42, 43]. For O_2/N_2 separation it can be noticed that **PI-6FDA** is farthest from the limit, compared with the other two polyimides. However, from the permeability/selectivity map for CO_2/CH_4 separation, it can be observed that **PI-6FDA** is placed closer to the upper bound line due to increased selectivity compared to the reference polymers.

Figure 7. Here

4. Conclusions

Based on the synthesis of a novel aromatic diamine containing a rigid benzofuran unit, a series of three aromatic polyimides were successfully prepared by the solution polycondensation technique and then structurally characterized. Polyimides with CF_3 bulky groups and diphenylsilane units were soluble in polar aprotic solvents at room temperature. All **PIs** were thermally stable and the Tg values were high, indicating an elevated structural rigidity. The presence of silicon atoms significantly affected the physical properties, and so, **PI-SiDA** showed a slightly lower Tg than **PI-BTDA** and **PI-6FDA** while **PI-SiDA** film was more hydrophobic than those of **PI-BTDA** and **PI-6FDA**. Gas transport properties were measured on the **PI-6FDA** with the aim to evaluate potential application on gas separation process. **PI-6FDA** showed lower permeability coefficients than related polyimides previously reported, but exhibited a significant increase of selectivity for the CO_2/CH_4 separation. Thus, this polyimide had a better performance than Matrimid to attain this separation.

5. Acknowledgements

Tundidor-Camba, A. acknowledges the financial assistance by Comisión Nacional de Investigación Científica y Tecnológica, CONICYT, through Project 79130011.

References

1 S. A. Stern, Y. Mi, H. Yamamoto, St. A. K. Clair. *J. Polym. Sci., Polym. Phys*. 1989, **27**, 1887.

2 K.Toi, H. Suzuki, I. Ikemoto, T. Ito, T. Kasai. *J. Polym. Sci., Polym. Phys.* 1995, **33**, 777.

3 K. L. Mittal. *Polyimides: Synthesis, Characterization, and Applications*; Plenum Press: New York, 1984.

4 M. K. Ghosh, K. L. Mittal. *Polyimides: Fundamentals and Applications*; Marcel Dekker, Inc.: New York, 1996.

5 C. L. Chung, S. H. Hsiao. *Polymer* 2008, **49**, 2476.

6 L. Tao, H. Yang, J. Liu, L. Fan, S. Yang. *Polymer* 2009, **50**, 6009.

7 S. H. Hsiao, H. M. Wang, J. S. Chou, W. Guo, T. M. Lee, C. M. Leu, C. W. Su. *J. Polym. Res.* 2012, **19**, 9757.

8 S. H. Hsiao, H. M. Wang, W. J. Chen, T. M. Lee, C. M. Leu. *J. Polym. Sci. Polym. Chem.* 2011, **49**, 3109.

9 M. Xiaohua, S. Raja, B. Youssef, Z. Yihan, L. Eric, J. Mustapha, P. Ingo, H. Yu. *Macromolecules* 2012, **45**, 3841.

10 M. Carta, R. Malpass-Evans, M. Croad, Y. Rogan, J. C. Jansen, P. Bernardo, F. Bazzarelli, N. B. McKeown, *Science* 2013, **339**, 303.

11 C. G. Bezzu, M. Carta, A. Tonkins, J. C. Jansen, P. Bernardo, F. Bazzarelli, N. B. McKeown, *Adv.Mater.* 2012, **24**, 5930.

12 N. Du, H. B. Park, G.P.Robertson, M. M. Dal-Cin, T. Visser, L. Scoles, M. D.Guiver, *Nat. Mater.* 2011, **10**, 372.

13 D. J. Liaw, N. Ueyama, A. Harada, *Macromolecular Nanostructured Materials*; Kodansha & Springer: Tokyo, Chapter, 2.2, 2004.

14 D. J. Liaw, C. W. Yu. *Polymer* 2001, **42**, 5175.

15 C. A. Terraza, J. G. Liu, Y. Nakamura, Y. S. Shibasaki, A. M. Ueda, *J. Polym. Sci. Part A: Polym. Chem.*, 2008, **46**, 1510.

16 A. Tundidor-Camba, C. A. Terraza, L. H. Tagle, D. Coll, I. Ojeda, M. Pino. *RSC Adv.*, 2015, **5**, 23057.

17 C. A. Terraza, L. H. Tagle, C. Contador, A. Tundidor-Camba, C. M. González-Henríquez, *Polymer Bulletin*, 2014, **71**, 1001.

18 M. Bruma, B. Schulz, *J. Macromol Sci. Polym Rev,* 2001, **41**, 1.

19 H. Behniafar, M. Ghorbani. *Polym Degrad Stab*., 2008, **93**, 608.

20 N. V. Sadavarte, M. R. Halhalli, C. V. Avadhani, P. P. Wadgaonkar. *Eur Polym J.*, 2009, **45**, 582.

21 J. de Abajo, J. G. de la Campa. *Adv. Polym. Sci.* 1999, **140**, 23.

22 H. S. Kim, Y. H. Kim, S. K. Ahn, S. K. Kwon. *Macromolecules* 2003, **36**, 2327.

23 M. Calle, A. E. Lozano, J. de Abajo, J. G. de la Campa, C. Álvarez. *J. Membr. Sci.* 2010, **365**, 145.

24 A. Suzuki, *Journal of Organometallic Chemistry*, 1999, **576**, 147.

25 J. R. Pratt, S. Thames. *J. Org. Chem.*, 1973, **38**, 4271.

26 A. Hilal, R. Steven, L. LaBrenz, L. Woo, C. Serpell, W. Jeffery, *J Am Chem Soc*., 2000, **122**, 5262.

27 L. H. Tagle, C. A. Terraza, A. Leiva, F. Devilat, *J Appl. Polym. Sci,* 2008, **110**, 2424.

28 C. A. Terraza, L. H. Tagle, F. Concha, L. Poblete, *Des. Monomers Polym.,* 2007, **10**, 253.

29 S.A. Stern, *J. Membr. Sci.* 1994, **94**, 1.

30 M.R. Coleman, W.J. Koros, *J. Polym. Sci. B: Polym. Phys.* 1994, **32**, 1915.

31 J. D. Wind, C. Staudt-Bickel, D. R. Paul, W. J. Koros. *Ind. Eng. Chem. Res*. 2002, **41**, 6139.

32 J. D. Wind, D. R. Paul, W. J. Koros, *J. Membr. Sci.* 2004, **228**, 227.

33 A. M. Hillock, W. J. Koros, *Macromolecules* 2007, **40**, 583.

34 I. C. Omole, S. J. Miller, W. J. Koros, *Macromolecules* 2008, **41**, 6367.

35 E. M. Maya, A. E. Lozano, J. de Abajo, J. G. de la Campa, *Polym. Degrad. Stab*. 2007, **92**, 2294.

36 O. Müller, A. Borisov, *Advance in polymer Science 242 Self Organized Nanostructures of Amphiphilic Block Copolymers II.*, Springer, 2011.

37 S. H. Wu. *J. Polym Sci Part C Polym Symp* 1971, **34**, 19.

38 T. Zhang, D. Y. Hu, J. H. Jin, S. L. Yang, G. Li, J. M. Jiang, *Eur Polym J* 2009, **45**, 302.

39 Y. Huang, D. R. Paul. *Industrial & Engineering Chemistry Research* 2007, **46**, 2343.

40 D. Q. Vu, W. J. Koros, S. J. Miller. *J. Membr. Sci* 2003, **211**, 311.

41 Y. Zhang, I. Musselman, J. Ferraris, Jr. K. J. Balkus. *J. Membr. Sci* 2008, **313**, 170.

42 L. M. Robeson, *J. Membr. Sci.* 1991, **62**, 165.

43 L. M. Robeson, *J. Membr. Sci.* 2008, **320**, 390.

List of figures and scheme captions

Scheme 1. Synthetic route to obtain 2,8-di(3-aminophenyl)dibenzofuran.

Scheme 2. Synthetic route of aromatic polyimides.

Fig. 1. FT-IR spectra (KBr pellet) of both dinitro (**1**) and diamine (**2**) compounds.

Fig. 2. ^{1}H and ^{13}C NMR spectra (400 MHz, DMSO-d_6) of aromatic diamine **2**.

Fig. 3. FT-IR spectra (KBr pellet) of **PI-SiDA**.

Fig. 4. ^{1}H and ^{29}Si NMR spectra (400 MHz, DMSO-d_6) of **PI-SiDA**.

Fig. 5. TGA curves of **PIs**.

Fig. 6. Profiles of a droplet on the **PIs**. **a) PI-6FDA (**water). **b) PI-6FDA** (toluene). **c) PI-SiDA** (water) and **d) PI-SiDA** (toluene).

Fig. 7. Performance of **PI-6FDA** O_2/N_2 (left) and CO_2/CH_4 (right) separations compared with other polyimides reported in the literature.

Tables.

Table 1. Inherent viscosity and solubility results of **PIs**.

		Solubility					
PI	η_{inh} (dL/g)[a]	DMSO	NMP	DMF	DMAc	*m*-cresol	THF
PI-6FDA	0.60	+	+	+	+	+	-
PI-BTDA	-	-	-	-	-	-	-
PI-SiDA	0.74	+	+	+	+	+	-

[a]Measured in NMP (0.5 g/dL at 25 °C) Solubility: +, Soluble at room temperature; -, Insoluble.

Table 2. Summary of thermal properties of the **PIs**.

PI	[a]$TDT_{10\%}$ (°C)	[b]Char Yield (%)	[c]Tg (°C)
PI-6FDA	555	65	315
PI-SiDA	580	80	290
PI-BTDA	590	45	300

[a]Thermal decomposition temperature at which 10 % weight loss was recovered by TGA at a heating rate of 10 °C/min in nitrogen atmosphere. [b]Residual weight (%) when heated to 800 °C. [c]Glass transition temperature taken at 10 °C/min in nitrogen atmosphere.

Table 3. Contact angle and surface free energy of soluble **PIs**.

PI	θ_w (°)[a]	θ_t (°)[b]	σ^c (mJ/m^2)	σ^d_d (mJ/m^2)	σ^e_p (mJ/m^2
PI-6FDA	75.4	61.6	33.0	14.2	19.7
PI-SiDA	80.2	79.9	32.8	9.6	23.2

[a]Contact angle recorded at a rate of 10 µL/s at 25 °C in water. [b]Contact angle recorded at a rate of 10 µL/s at 25 °C in toluene. [c]Total surface free energy. [d]Dispersive component. [e]Polar component.

Table 4. Gas transport properties of **PI-6FDA**.

	Permeability (barres)[a]				Ideal separation factors	
PI	**CO_2**	**O_2**	**N_2**	**CH_4**	**O_2/N_2**	**CO_2/CH_4**
PI-6FDA	8.7	2.4	0.4	0.2	6.0	43.5
6FDA-TBAPB[b]	65.6	16.5	3.5	2.9	4.6	22.1
Matrimid[c]	10.0	2.1	0.3	0.3	7.0	33.3

[a]1 barrers = 10^{-10} cm^3 (STP) cm/(s cm^2 cmHg). [b]Reference 23. [c]Reference 39-41.

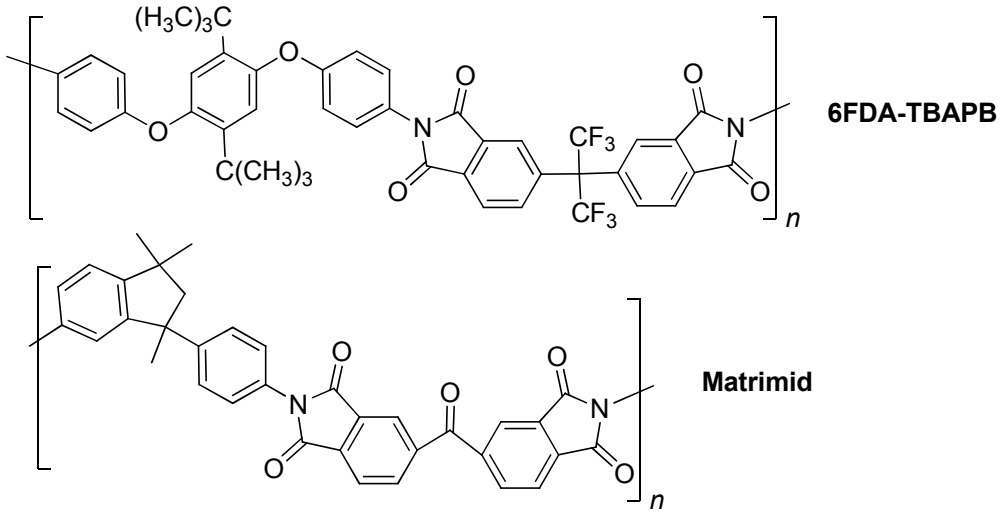

6FDA-TBAPB

Matrimid

Schemes and figures

Scheme 1.

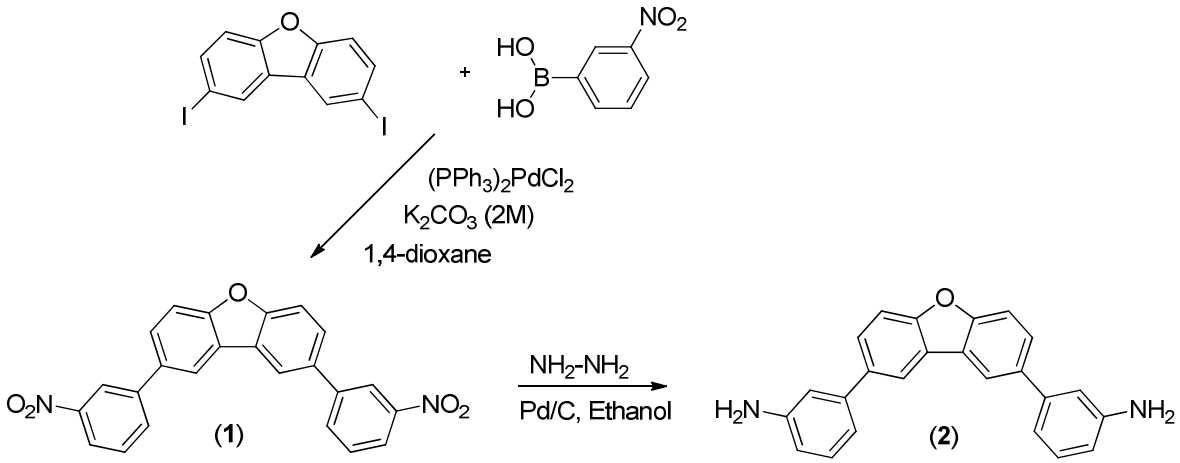

Scheme 2.

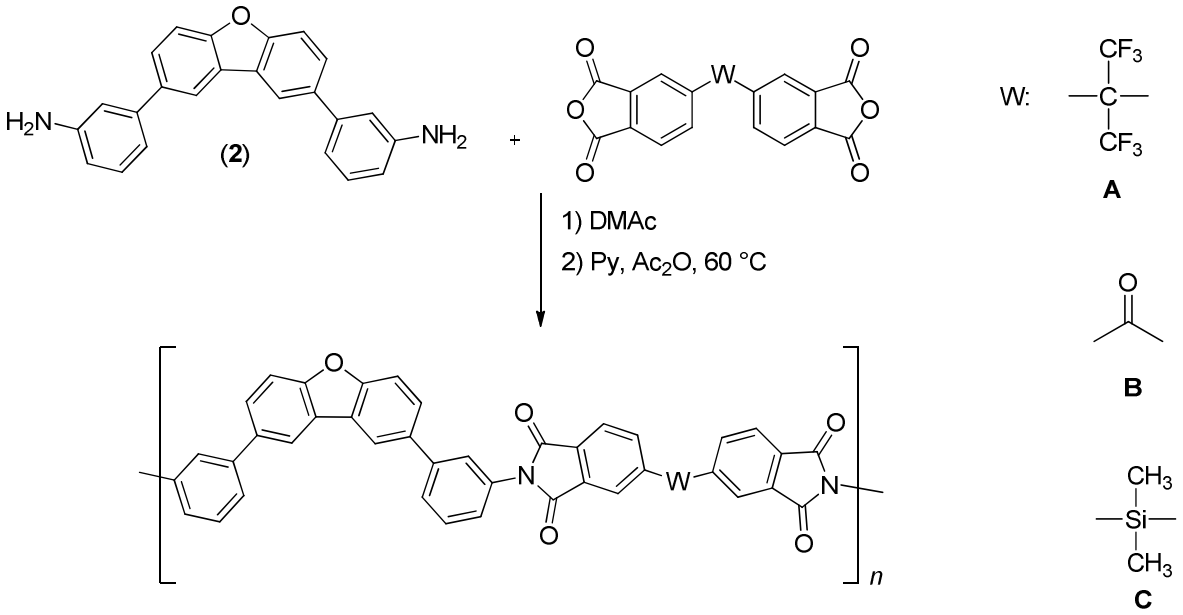

PI-6FDA: 2-A; PI-ODA: 2-B; PI-SiDA: 2-C

Figure 1.

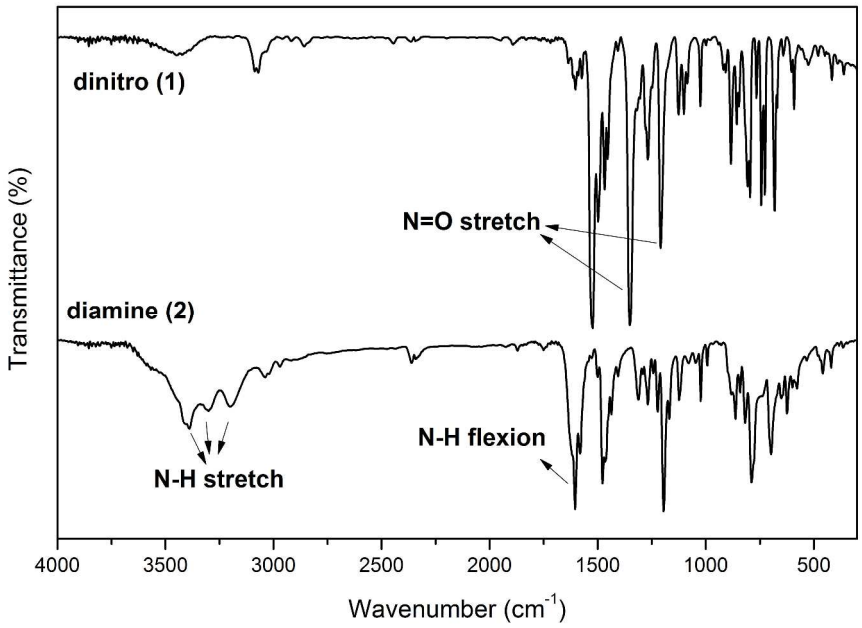

Figure 2.

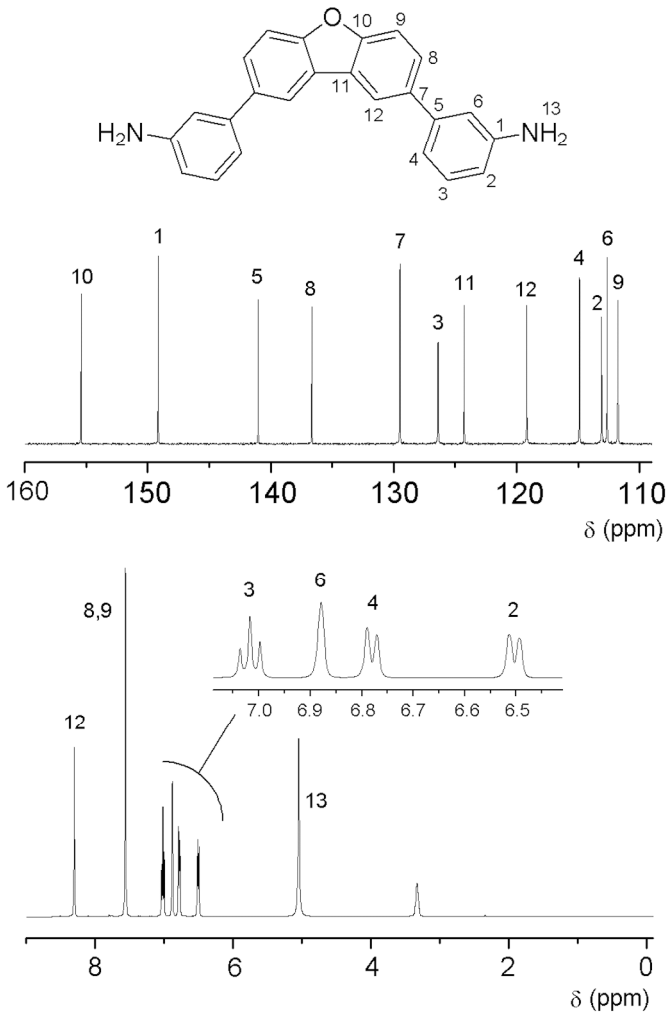

Figure 3.

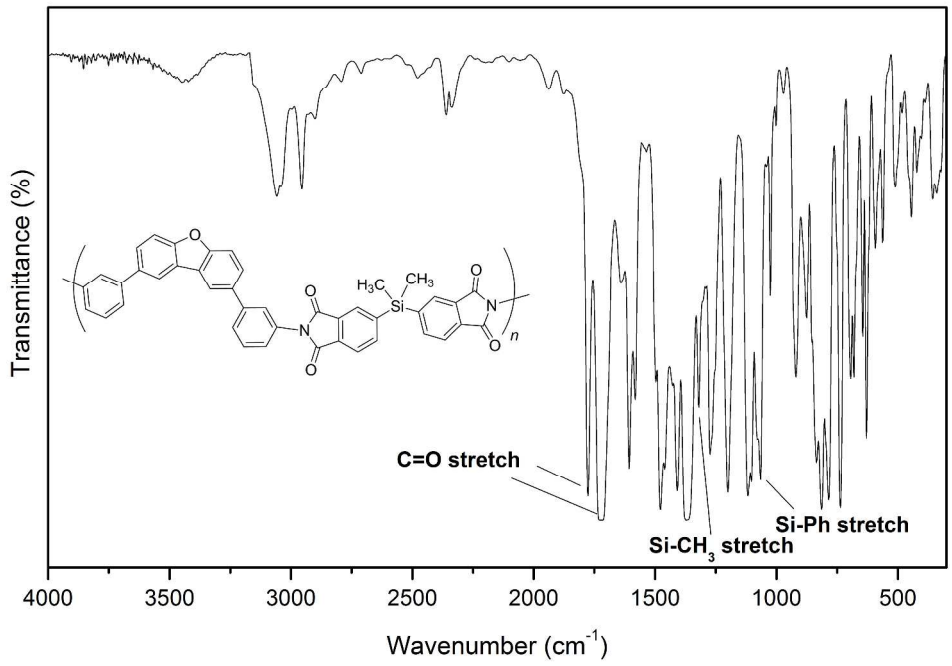

Figure 4.

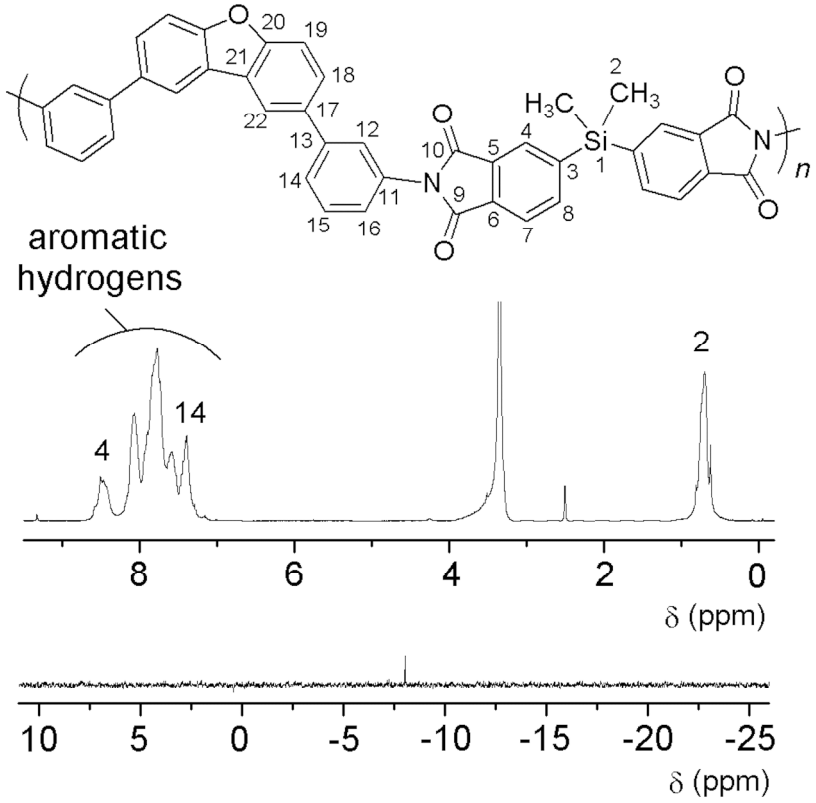

Figure 5.

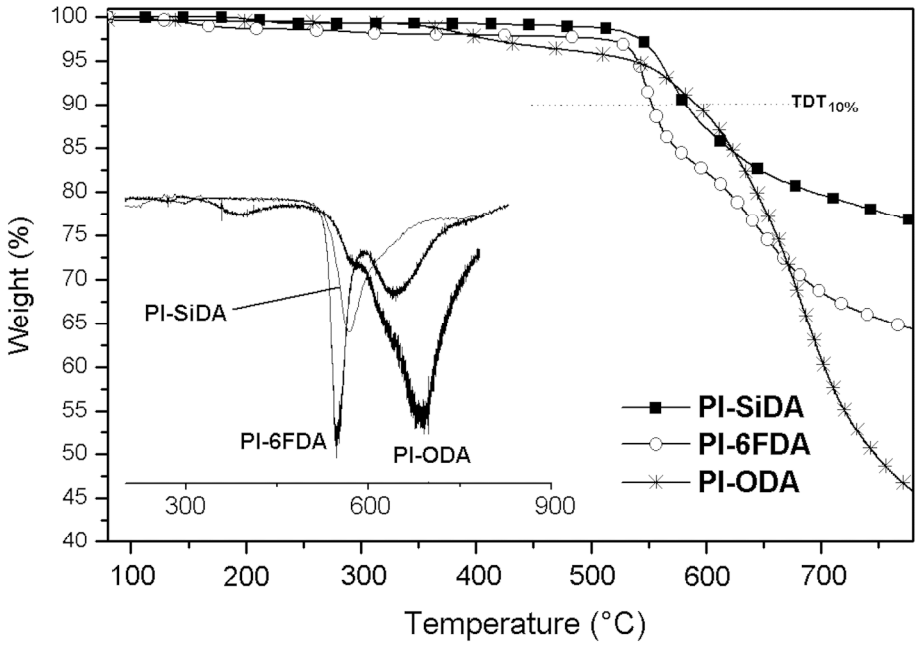

Figure 6.

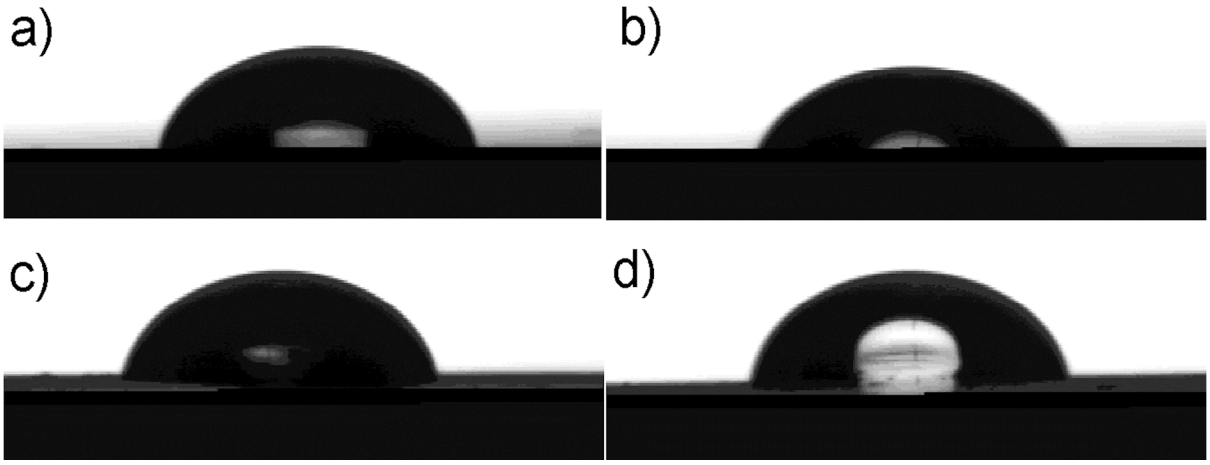

Figure 7

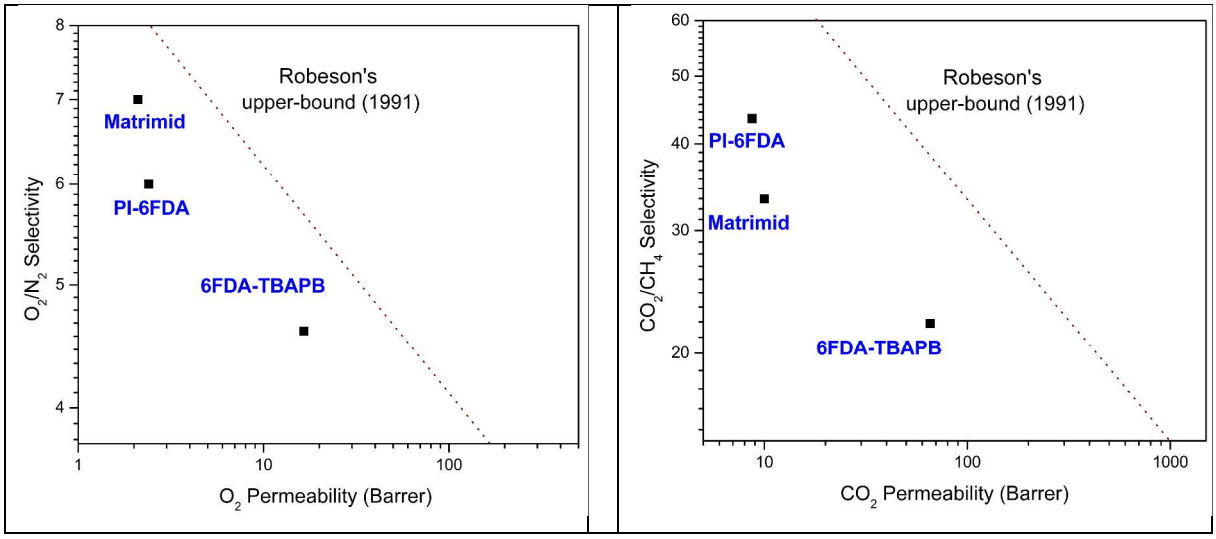

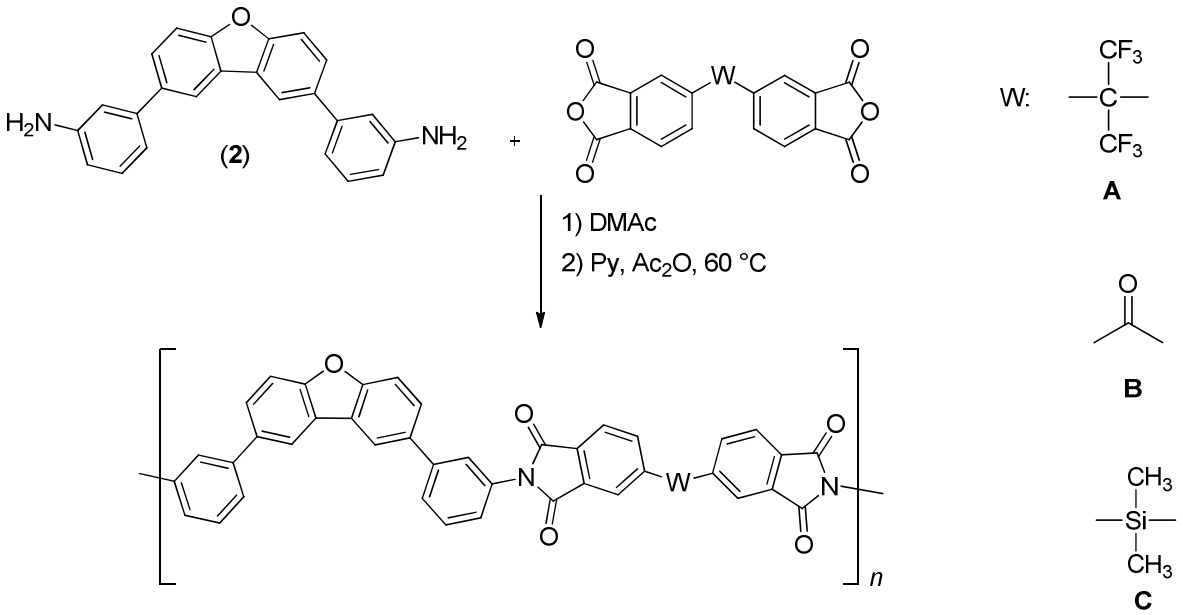

PI-6FDA: 2-A; PI-ODA: 2-B; PI-SiDA: 2-C

Graphical Abstract